

MIT Open Access Articles

*Estimating the Number of Stable Configurations
for the Generalized Thomson Problem*

The MIT Faculty has made this article openly available. **Please share** how this access benefits you. Your story matters.

Citation: Calef, Matthew, Whitney Griffiths, and Alexia Schulz. "Estimating the Number of Stable Configurations for the Generalized Thomson Problem." *Journal of Statistical Physics* 160.1 (2015): 239–253.

As Published: <http://dx.doi.org/10.1007/s10955-015-1245-6>

Publisher: Springer US

Persistent URL: <http://hdl.handle.net/1721.1/104900>

Version: Author's final manuscript: final author's manuscript post peer review, without publisher's formatting or copy editing

Terms of Use: Article is made available in accordance with the publisher's policy and may be subject to US copyright law. Please refer to the publisher's site for terms of use.



Estimating the Number of Stable Configurations for the Generalized Thomson Problem

Matthew Calef¹ · Whitney Griffiths² · Alexia Schulz³

Received: 5 November 2014 / Accepted: 24 March 2015 / Published online: 31 March 2015
© Springer Science+Business Media New York 2015

Abstract Given a natural number N , one may ask what configuration of N points on the two-sphere minimizes the discrete generalized Coulomb energy. If one applies a gradient-based numerical optimization to this problem, one encounters many configurations that are stable but not globally minimal. This led the authors of this manuscript to the question, how many stable configurations are there? In this manuscript we report methods for identifying and counting observed stable configurations, and estimating the actual number of stable configurations. These estimates indicate that for N approaching two hundred, there are at least tens of thousands of stable configurations.

Keywords Many-body systems · Stability · Unseen species

1 Introduction

Computer trials indicate that in the range $70 \leq N \leq 112$, the number of distinct configurations associated with each value of N grows exponentially, i.e., $M(N) = 0.382 \exp(0.0497N)$. If this trend is sustained for larger values of N , identifying global minima among a large set of nearly degenerate states for complex systems of this type will pose formidable technical challenges. Erber and Hockney [7]

For a natural number N , we denote by $\omega_N = \{\mathbf{r}_1, \dots, \mathbf{r}_N\}$ any configuration of N distinct points on \mathbb{S}^2 . For a non-negative number s , one can ask what configuration minimizes the energy

✉ Matthew Calef
mcalef@lanl.gov

¹ Computational Physics and Methods, Los Alamos National Laboratory,
Los Alamos, NM 87545-0001, USA

² Financial Institutions Group, Bank of America, New York, NY 10036, USA

³ Cyber Security and Information Sciences, MIT Lincoln Laboratory, Lexington,
MA 02420-9108, USA

$$E_s(\omega_N) := \sum_{i=1}^{N-1} \sum_{j=i+1}^N k_s(|\mathbf{r}_i - \mathbf{r}_j|), \quad \text{where } k_s(r) = \begin{cases} r^{-s} & \text{when } s > 0 \\ -\log r & \text{when } s = 0. \end{cases}$$

For $s = 1$ this is known as the Thomson Problem [23]. At first glance this problem seems remarkably simple, yet there is not a simple solution. In fact, Smale has identified a variant of this problem as worthy of focus for this century [21].

The current theoretical progress is limited. It is known that for any N and s a globally minimal configuration exists. For a few special cases of N and s there are rigorous proofs that certain configurations are globally minimal. Finally, there are some asymptotic estimates for the minimal energy as a function of N . In this last category Pólya and Szegő [20], using measure-theoretic arguments, established some elegant estimates when s is less than the dimension of the set on which the problem is posed, e.g., 2 in the case of \mathbb{S}^2 (also cf. Landkof [16, pp. 160–162]). Hardin and Saff [11], and Borodachov, Hardin and Saff [2] established similar results when s is greater than or equal to the dimension of the set in question.

While theoretical progress is difficult, the analyticity of k_s makes this an inviting problem for numerical optimization, particularly gradient-based optimizations. Work in this area goes back to at least 1977 [18], and there are two efforts that particularly motivated this current effort. The first is Erber's and Hockney's reports and commentary [6–8] on computational experiments for the Thomson problem for N up to 65 and N up to 112, where they provide some initial estimate for the growth in the number of stable configurations as a function of N . This work also includes estimates for the first two terms in the asymptotic expansion for the minimal energy. The first term is in agreement with the earlier work of Pólya and Szegő, and the second term was later identified in a formal conjecture by Kuijlaars and Saff [14] and later generalized to a large class of two-manifolds [3]. The second effort is the work by Wales and Ulker [24], and the work by Wales, McKay and Altschuler [25] that led to the Cambridge Cluster Database, which reports, for many N and $s = 1$, the lowest known energy for the Thomson problem.

A significant challenge for numerical optimization is that many configurations are locally minimal, i.e. stable, with respect to E_s , but not globally minimal. This motivated us to attempt to answer the question: how many stable configurations for a given N and s are there? An earlier work that answers a similar question is that of Hoare and McInnis, who identify the distinct stable clusters of modest numbers of point-particles interacting through Lennard-Jones and Morse potentials [13]. For the Lennard-Jones potential the number of stable clusters grew rapidly. The present work estimates this growth for the generalized Thomson problem for N up to 180 and for $s = 0, 1, 2$, and 3, and reports some methods we found useful.

A central question is whether the number of distinct local minima within the energy landscape grows exponentially with the number of points. Stillinger and Weber present the following informal argument suggesting an affirmative answer [22, p. 980]. If one can convert one stable configuration into another with changes that are localized in space to within a fixed number nearest neighbor lengths, then, as the number of points grows, so should the number of available independent changes, and the number of stable configurations grows will grow exponentially. If the number of stable configurations does not increase exponentially with N , then this would suggest that changes from one stable configuration to another cannot be accomplished with only localized changes.

Our work began by generating a large library of stable configurations, and we describe our methods in Sect. 2. In doing this, we found that our optimization program would find rotations and reflections of the same stable configuration. In response, we used graph-isomorphisms of the Delaunay triangulation as a means to recognize quickly a particular stable configuration.

This method accelerated our work considerably, but there are some subtle ways it can fail. In particular we found two distinct stable configurations whose Delaunay triangulations share the same graph structure. This is described in Sect. 3. Even after months of numerical experiments running on many compute cores, the fraction of the most recent experiments that generated new configurations never dropped to zero, making it clear that there are many stable configurations we did not see. The problem of estimating the number of configurations we didn't see is an example of the broader "unseen species" problem, which arises in many settings such as linguistics and ecology. We apply a method developed partly by linguists to provide estimates in Sect. 4 for the actual number of stable configurations.

2 Stable Configurations

2.1 Optimization

We used an iterative unconstrained optimization strategy described in Sect. 3.1 of our prior work[3] to generate candidate stable configurations. The method consists of non-linear conjugate gradient (NLCG) with line minimization and, when that method no longer made progress, Newton's Method. Our experience is that NLCG with line minimization was most effective up until near the end of the optimization. Near the end of the optimization calculation, presumably when the configuration is at a point where the objective function E_s is locally quadratic, Newton's Method would often make progress when NLCG could not.

When computing the energy, $E_s(\omega_N)$, one has roughly $N^2/2$ summands that vary widely in range, and a direct summation can lead to roundoff errors. We controlled for this error by logarithmically binning our summands and only adding the content from the same bin. This allowed us to ensure that we never added two numbers whose ratio was more than two or less than one half, until the end when we summed the contents of the bins from lowest to highest. Because we could bound the error for summation in a given bin, and because we could count the number of summations in the bin, we were able to estimate the error in our sums. This approach follows the work of Higham [12] and Demel and Hida [4].

2.2 Testing for Stability

Given a candidate stable configuration, we use the criteria described in Sect. 3.2 of a previous publication [3] to test for stability. The central assumption in this criteria is that our iterative optimization strategy will produce a candidate configuration ω_N^c that is close enough to an actual stable configuration $\bar{\omega}_N$, so that the gradient at $\bar{\omega}_N$, which is zero, may be expressed as a linear expansion of the gradient about ω_N^c . That is

$$0 = \nabla E_s(\bar{\omega}_N) \approx \nabla E_s(\omega_N^c) + \nabla^2 E_s(\omega_N^c)(\bar{\omega}_N - \omega_N^c), \tag{1}$$

where ∇E_s and $\nabla^2 E_s$ are the gradient and the Hessian respectively of the objective function with respect to the $2N$ angular free parameters. If this approximation were exact, it would allow us to bound the term $\bar{\omega}_N - \omega_N^c$, where subtraction is applied to the $2N$ -dimensional space of configurations. Conceptually the calculation is

$$-\nabla^2 E_s(\omega_N^c)^{-1} \nabla E_s(\omega_N^c) = (\bar{\omega}_N - \omega_N^c),$$

$$\|\nabla^2 E_s(\omega_N^c)^{-1}\|_2 \|\nabla E_s(\omega_N^c)\|_2 \geq \|\bar{\omega}_N - \omega_N^c\|_2 \geq \|\bar{\omega}_N - \omega_N^c\|_\infty.$$

Here $\|\cdot\|_2$ is the unnormalized two-norm allowing the bound of the infinity-norm.

The Hessian is not invertible, however. For our choice of coordinates there are three rotations of the sphere that do not change the relative distance between the points and hence don't change the energy. While there are choices of coordinates free of such rigid rotations, those coordinate systems degraded the performance of NLCG. Consequently the three lowest eigenvalues of the Hessian are zero. The gradient has no projections along the corresponding eigenvectors, and we may choose a rotation of $\bar{\omega}_N$ so that the difference $\bar{\omega}_N - \omega_N^c$ similarly does not project along these eigenvectors. We let λ_{\min}^* denote the fourth lowest eigenvector of the Hessian and then we have

$$\frac{\|\nabla E_s(\omega_N^c)\|_2}{\lambda_{\min}^*} \geq \|\bar{\omega}_N - \omega_N^c\|_2 \geq \|\bar{\omega}_N - \omega_N^c\|_\infty.$$

Change in angle on the sphere bounds from above change in position, and so $\|\bar{\omega}_N - \omega_N^c\|_\infty$ provides a bound on the distance between corresponding points in the configurations $\bar{\omega}_N$ and ω_N^c .

Our criteria for stability is that

$$\frac{\|\nabla E_s(\omega_N^c)\|_2}{\lambda_{\min}^*} \leq \frac{\min_{\mathbf{r}_i \neq \mathbf{r}_j \in \omega_N^c} |\mathbf{r}_i - \mathbf{r}_j|}{10,000}, \tag{2}$$

which, in conjunction with the assumption that error in the approximation in Eq. (1) is negligible, leads to the conclusion that no point in ω_N^c is further from the corresponding point in $\bar{\omega}_N$ by more than one ten-thousandth the minimum pairwise separation of the points in ω_N^c . An important consequence of this is that if two configurations satisfy Eq. (2), and if there is a rotation and reflection that aligns them to within one five-thousandth of both of their minimum pairwise distances, then, we say that they are instances of the same stable configuration. As previously noted [3] this criteria relies on bounding the infinity-norm with the unnormalized 2-norm. Such a bound is tight only when all the components except one are zero. The implication is that the maximum difference between a point in our candidate configuration and a true stable configuration is likely considerably less than one ten-thousandth of the minimum pairwise separation of the points within the configuration in question. For candidate configurations that we believed were instances of the same stable configuration, we could often align them to greater accuracy.

The condition in Eq. (2) is a useful, reasonably motivated, heuristic for marking a configuration as stable. More rigorous bounds would require estimating the error in Eq. (1).

3 Delaunay Triangulations and Graph Isomorphisms

Since the energy E_s depends only on the distances between points, it is invariant under isometry. However, that two configurations of points have the same energy does not ensure that there is an isometry between the two configurations. With this in mind we only called two configurations the same if we could find an isometry that mapped one configuration onto the other to within the tolerances described in the previous section.

This leaves the question of how to search for an isometry between two configurations of similar energy, which we'll denote here as $\omega_N^1 = \{\mathbf{s}_1, \dots, \mathbf{s}_N\}$ and $\omega_N^2 = \{\mathbf{r}_1, \dots, \mathbf{r}_2\}$. A simple approach is to apply Algorithm 1 described in this manuscript. While there are some optimizations such as, at line 5, first testing that $|\mathbf{r}_i - \mathbf{r}_j| = |\mathbf{s}_1 - \mathbf{s}_2|$, this algorithm is expensive and must be applied to every pair of configurations with similar energy.

Algorithm 1 A simple way to search for isometries between ω_N^1 and ω_N^2 .

```

1: Isometry Found  $\leftarrow$  False.
2:  $\varepsilon \leftarrow 2 \min \left\{ \frac{\min_{s_i \neq s_j \in \omega_N^1} |s_i - s_j|}{10,000}, \frac{\min_{r_i \neq r_j \in \omega_N^2} |r_i - r_j|}{10,000} \right\}$ 
3: for  $r_i \in \omega_N^2$  do
4:   for  $r_j \in \omega_N^2 \setminus \{r_i\}$  do
5:     if there is a rotation of  $\omega_N^2$  so that  $r_i = s_1 \in \omega_N^1$  and so that  $r_j = s_2 \in \omega_N^1$  to within  $\varepsilon$  then
6:       if this rotation is such that  $\|\omega_N^1 - \omega_N^2\|_\infty < \varepsilon$  then
7:         Isometry Found  $\leftarrow$  True.
8:       else
9:          $\tilde{\omega}_N^2 \leftarrow$  the reflection of the rotation of  $\omega_N^2$  about the plane defined by  $s_1, s_2$  and  $\mathbf{0}$ .
10:      if  $\|\omega_N^1 - \tilde{\omega}_N^2\|_\infty < \varepsilon$  then
11:        Isometry Found  $\leftarrow$  True.
12:      end if
13:    end if
14:  end for
15: end for
16: end for

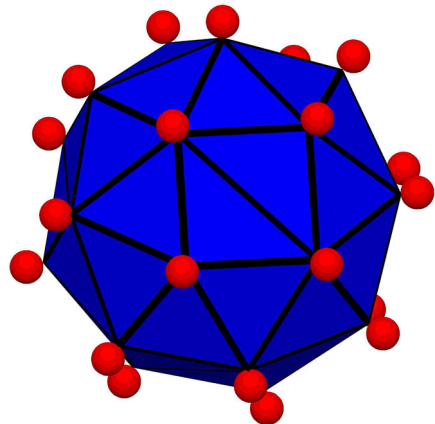
```

3.1 Delaunay Triangulations

We found a more effective algorithm was to look for isomorphisms between the graphs formed from the extremal edges in the Delaunay Triangulations of the configurations in question. For brevity we shall refer to this as an extremal triangulation. Essentially we are looking at the edges in the set of triangles that make up the surface of the smallest polyhedron containing a configuration, ω_N .

To compute the extremal triangulation we used the QHULL software package [1]. One immediate observation was that certain configurations did not have unique extremal triangulations, for example, the configuration with the lowest observed energy for $N = 24$ and $s = 1$, shown in Fig. 1. The four points displayed toward the middle of the image are the vertices of a square, and either diagonal can be part of a valid extremal triangulation. Because there can be degenerate extremal triangulations, the assumption that distinct extremal trian-

Fig. 1 This is one of many possible extremal triangulations for this configuration of 24 points



gulations indicate non-isometric configurations is not, in general, correct. A simple test for non-degeneracy is to compute the set of unit normal vectors for the extremal faces, and to make sure that the dot-product of any two is bounded away from one.

In the case that a configuration has a non-degenerate extremal triangulation, the edges of the triangulation and the points in the configuration form a graph, and this graph is invariant under rotation and reflection of the underlying configuration. In the degenerate case, a rotation or reflection may lead QHULL, due to round-off errors, to find a different, but equally valid, extremal triangulation.

3.2 Graph Isomorphisms

A graph on a sphere is a planar graph in that, by choosing one face to be mapped to the unbounded component of the plane, the graph can be mapped onto the plane. In doing this the edges that bound this face are retained, and the graph structure is preserved whether the graph is embedded on \mathbb{S}^2 or \mathbb{R}^2 . There are efficient algorithms to determine isomorphisms of planar graphs and we use one following the work of Lins [17]. The approach is to generate a tag for each graph with the property that two graphs are isomorphic if, and only if, the two tags are the same. The cost for finding isomorphisms between M instances of graphs, or for finding isometries between M configurations, can be written as

$$C_1M + C_2M^2.$$

In our approach C_2 is the cost of a searching for matching tags, i.e. string comparisons, while C_1 is the cost of generating the tag. For large M , this has substantial benefits, over the case that C_1 is zero, but C_2 is the cost associated with Algorithm 1.

The specific method we use for generating a tag is given in Algorithm 2. We denote our graph as a set of vertices V and a set of edges E , and for any $v \in V$ we denote by $E(v)$ the set of edges that have v as an endpoint. To each vertex v we assign a natural number i_v . The central idea in Algorithm 2 is to search for the lexically lowest encoding of a representation of the connectivity matrix, where we are searching over a set of possible orderings of vertices. We used an MD5 hash of the connectivity matrix simply to use less memory. The requirement that the graph be planar is what allows us to generate the unique ordering of W at line twelve. We stored the configuration with the ordering of points that generated the lexically lowest encoding, i.e. the tag.

When we generated a new stable configuration for a given N and s we would, when the new configuration had a non-degenerate extremal triangulation, also generate the associated tag. We would then collect the already generated configurations for that N and s whose energies were close to the energy of the newly generated configuration. Within the subset of these with unique extremal triangulations, we would search for the tag associated with the new configuration. If we found it, then because we stored the configurations with the orderings of points that generated the tag, we knew the rotation and reflection necessary that would be the isometry. It was our experience that, when there was an isometry, this method found it immediately. Further, it was our experience that almost all of the configurations had non-degenerate extremal triangulations.

If we did not find matching tags, then we used Algorithm 1 to search for an isometry between the newly generated configuration and the existing configurations with similar energies. We only characterized a configuration as new for a given N and s if every configuration with that N and s had an energy that was sufficiently different to ensure that there was no isom-

Algorithm 2 Generating a tag for a planar graph.

```

1: Tag  $\leftarrow$  None.
2: for  $v \in V$  do
3:   for  $e \in E(v)$  do
4:     for  $r \in \{\text{Clockwise, Counterclockwise}\}$  do
5:       Reset all indices  $i_v$  for  $v \in V$ .
6:        $i_v \leftarrow 1$ .
7:        $i_w \leftarrow 2$ , where the edge  $e$  joins the points  $v$  and  $w$ .
8:        $n \leftarrow 3$ .
9:       while there is a vertex that has not been indexed do
10:         $x \leftarrow$  the vertex with the lowest index that has an unindexed neighbor.
11:         $y \leftarrow x$ 's neighbor with the lowest index.
12:         $W \leftarrow$  set of neighbors of  $x$  ordered by  $r$  and starting with  $y$ .
13:        for  $w \in W$  do
14:          if  $w$  has not been indexed then
15:             $i_w \leftarrow n$ .
16:             $n \leftarrow n + 1$ .
17:          end if
18:        end for
19:      end while
20:       $P \leftarrow$  the connectivity matrix of the graph where the vertices are ordered by their indexing.
21:       $T \leftarrow$  the MD5 cryptographic hash of  $P$ .
22:      if Tag = None or  $T <$  Tag then
23:        Tag  $\leftarrow T$ .
24:      end if
25:    end for
26:  end for
27: end for

```

etry or that the application of Algorithm 1 did not find an isometry. The graph-isomorphism technique sped the process of finding isometries when they existed, but it was never used by itself to determine if a configuration was new or isometric to an existing one.

There are two reasons why one should not rely exclusively on isomorphisms of non-degenerate extremal triangulations. The first is that it is possible, although we didn't see this case, that the graph has a non-trivial automorphism, but that the associated mapping of points is not a self-isometry. Put another way, there may be two orderings of the points that lead to the same lexically minimal tag. An indication of this would be that, at line twenty-two of Algorithm 2, Tag was not None and $T = \text{Tag}$, but, that there is no isometry between the configurations that preserves the orderings of points. An extremely simple example is a triangle where no two sides have the same length. It has no self-isometries, but six graph-automorphisms. Also, there is the remote possibility for collisions in the MD5 algorithm.

The more significant reason that graph isomorphisms alone are not sufficient to identify stable configurations is that we found two distinct configurations that both have non-degenerate extremal triangulations, but whose graphs were isomorphic. For $N = 102$ and $s = 2$, the configurations with the fourth and fifth lowest energy have non-degenerate extremal triangulation with isomorphic graphs. The dual graphs, i.e. the Voronoi cells, are shown in Fig. 2. The difference in energy is substantially more than the estimated error in the energy sums. The energies are 5582.2331644897 and 5582.2332117851 respectively. Algorithm 1 did not identify an isometry. Further, out of thousands of computer trials, we reproduced the fourth lowest configuration 205 times and the fifth lowest configuration 100 times—these were not rare configurations.

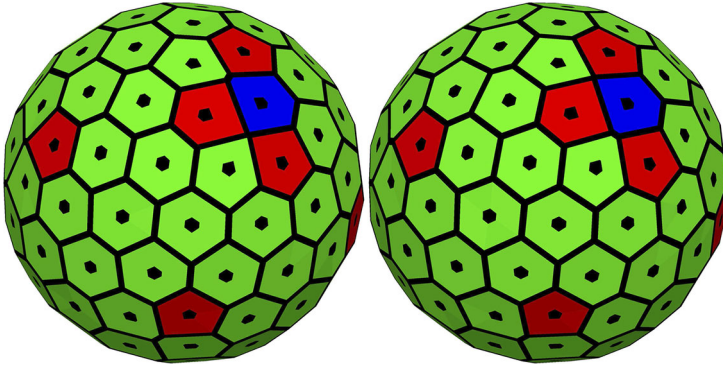


Fig. 2 On the *left* is the configuration with the fourth lowest energy for $N = 102$ and $s = 2$, on the *right* is the configuration with the fifth lowest energy. They have the non-degenerate extremal triangulation with isomorphic graphs, but are distinct stable configurations. The *dark* (blue in the online version) cell has seven edges, two of which in the *upper left* and *lower left* are extremely short. The reader will notice that these two edges differ in the image on the *left* and the *right*

4 Unseen Species

After months of running on many compute cores, we found that for most N between 120 and 180 the rate at which we discovered new stable configurations was still far from zero. We took this as an indication that more trials would result in more distinct stable configurations, and that we had not seen all of them. In response, we aimed to estimate the number of stable configurations that we didn't see in our trials. Such an estimate cannot be made without additional assumptions, which we shall make clear as we proceed. There is some precedent for trying to estimate the number of unseen species. For example, Efron and Thisted estimated the number of words Shakespeare knew [5], although their approach is more sophisticated than ours.

In broad terms our approach is as follows: We first compute the Good–Turing frequency described below. This is an estimate for the combined probability of all the configurations we did not see. In addition this method produces estimated probabilities for the S stable configurations we did see, $\{p_1, p_2, \dots, p_S\}$. We assume that when these estimated probabilities are sorted in decreasing order the tail has a certain analytic form, i.e. that there is a $p(n)$ so that $p_n = p(n)$ for large n . We obtain $p(n)$ from the data, and use it to compute how many more configurations we would need for the sum of the probabilities of those unseen configurations to agree with the Good–Turing frequency.

The first assumption is that the number of stable configurations is finite. While this seems intuitively true, the function $f(x) = x \sin(1/x)$ for $x \neq 0$ and 0 for $x = 0$ has infinitely many local minima on the closed unit interval, indicating that a proof that there are finitely many stable configurations will depend on domain specific information.

A second assumption is that, were we to use a different gradient based optimization technique, the estimated probabilities for configurations we observed wouldn't be so different as to change dramatically the estimates for the unseen species. While we have no proof, our instincts are that the basins of attraction for gradient descent methods all are qualitatively the same, and that the initial random configurations were sufficiently disordered so as not to be "nearer" a particular subset of stable configurations. Indeed, efforts to avoid the preponderance of stable configurations while searching for the global minimum has lead researchers

away from purely gradient-based methods such as the work by Morris et al. [19], and the work by Lakhah and Bernoussi [15].

We now briefly summarize I. J. Good’s description of the Good–Turing estimate [10]. Suppose we perform T trials where we observed some number of distinct species—stable configurations in our case. We let n_r denote the number of species that we observed r times, and so

$$\sum_{r=1}^{\infty} n_r r = T. \tag{3}$$

We then ask, for a species that we saw r times, what is a reasonable estimate for the fraction of the population that consists of that species? The most straightforward estimate, r/T , has the drawback that the sum of the fractions is one, i.e. this estimates assumes that there were no unseen species. This is almost certainly wrong in our case. If the likelihood of seeing each species is described by a binomial distribution, which is reasonable in our case, Good arrives at the following estimate [10, Sect. 2, Eq. 15] for the probability of a species that was observed r times

$$\frac{r + 1}{T + 1} \frac{\mathcal{E}_{T+1}(n_{r+1})}{\mathcal{E}_T(n_r)}.$$

Here, in a slight abuse of notation, $\mathcal{E}_T(n_r)$ indicates the expectation value for the number of species that we would expect to see r times in T trials. To be applicable, Good makes the following approximation

$$\mathcal{E}_{T+1}(n_{r+1}) \approx n'_{r+1}, \quad \frac{T + 1}{T} \approx 1,$$

where n'_r is the smoothed number of species seen r times. The need for smoothing arises because at large r , i.e. for species that occurred many times, the discreteness of the measurement n_r within T trials becomes apparent. Gale and Sampson provide a method, which we used, for smoothing the data [9]. Figures 1 and 2 in that publication make clear the need for, and effect of, smoothing. The result is the following estimate for the probability of a species (configuration) that occurred r times in T trials [10, Eqs. 2, 2']

$$p_r = \frac{r + 1}{T} \frac{n'_{r+1}}{n'_r}$$

The estimated probability of all species that occurred r times, denoted \tilde{p}_r , is

$$\tilde{p}_r = \frac{r + 1}{T} n'_{r+1}$$

Summing these estimated probabilities over all observed species [10, Eqs. 7, 8] gives

$$\sum_{r=1}^{\infty} \tilde{p}_r = \frac{1}{T} \sum_{r=1}^{\infty} n'_{r+1}(r + 1) = \frac{1}{T} \left(\sum_{r=1}^{\infty} n'_r r - n'_1 \right).$$

If the smoothing process is performed so that Eq. (3) holds with n_r replaced with n'_r , then the combined probability of all of our observed species is given by

$$\frac{1}{T} (T - n'_1) = 1 - \frac{n'_1}{T}$$

and so the estimate for the probability of the unseen species is

$$p_0 = \frac{n'_1}{T}.$$

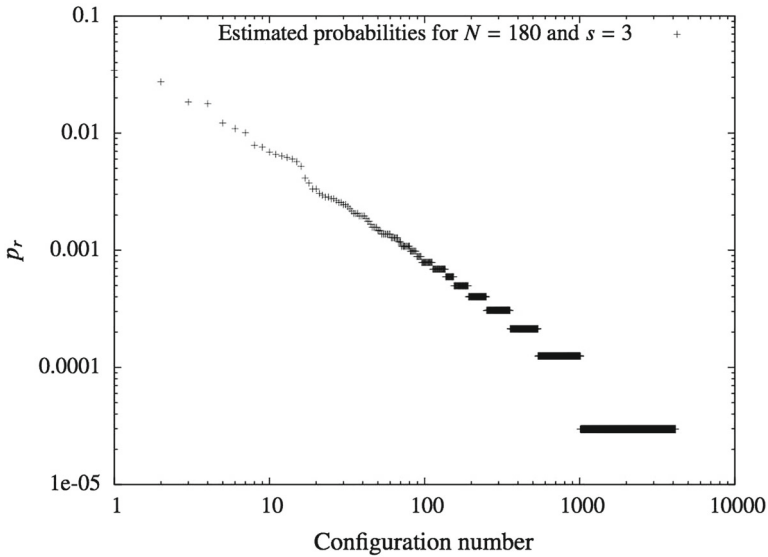


Fig. 3 This plot shows the estimated probability for all of the observed configurations, ordered in decreasing probability

This method gives us estimated probabilities for each of the configurations we have observed. For $N = 180$ and $s = 3$ we show these estimated probabilities in Fig. 3. The stair-step nature for the low estimated probabilities is an artifact of the finite number of samples. The estimated probability for a configuration depends only on the number of times the configuration occurred. This number can only be $1, 2, \dots$. Gale and Sampson’s smoothing technique addresses a similar problem, in that the observed values of n_r for large r must also be integral. We use a simple smoothing technique where, for a given probability, we take the geometric mean of the first and last configuration number as an estimate for the configuration number where that probability would occur. This is shown in Fig. 4.

We fit $Ax + \log b$ to the log–log tail of these data excluding the point corresponding to the configurations that occurred once. We are operating on two assumptions here: first, the tail of the probability distribution can be approximated $p(n) \approx bn^A$, and second, that the last point in Fig. 4 is not “below” the fit line, as much as it is “to the left” of the fit line. That is to say, for this sample, we believe that many more unseen configurations whose probability is close to p_1 than there are unseen configurations whose probability is close to or higher than p_2 .

Another statement of this assumption is that nearly all the unseen configurations have probability less than p_2 , but not necessarily less than p_1 .

With this in mind we solve the following for T_f

$$p_0 + n_1 p_1 = \int_{T_i}^{T_f} bn^A dn, \tag{4}$$

where p_0 is the estimated combined probability of all the species we didn’t see, p_1 is the estimated probability for the species we saw once, n_1 is the number of species that we saw once, and T_i is the number of configurations we saw at least twice. Note that we are only guaranteed to get a value of T_f if $A \geq -1$. When we apply this method we get an estimate

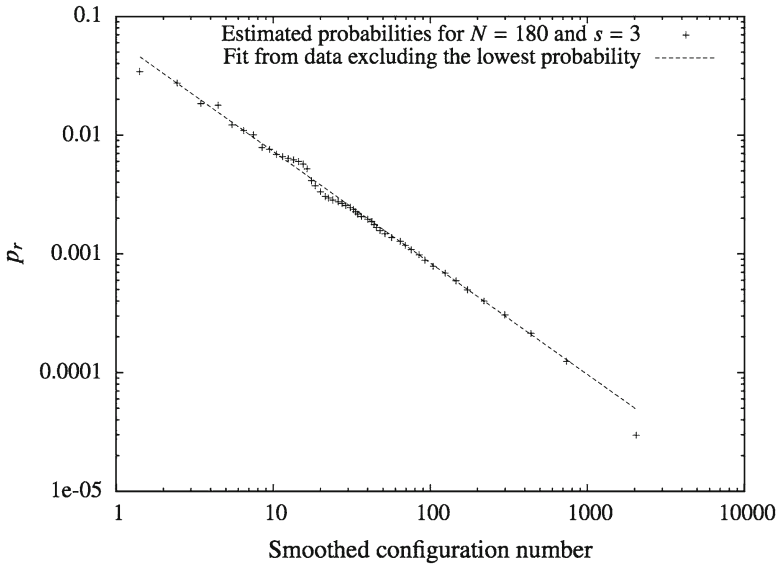


Fig. 4 This plot shows the smoothed estimated probability for all of the observed configurations

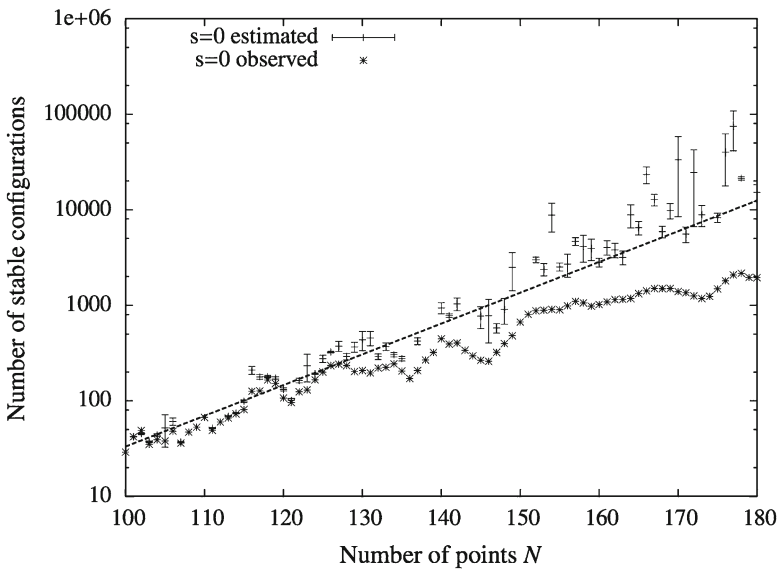


Fig. 5 The number of observed distinct stable configurations and estimates for the total number of distinct stable configurations as a function of N for $s = 0$

for the total number of stable configurations. These estimates as a function of N are plotted in Figs. 5, 6, 7 and 8 for $s = 0, 1, 2$ and 3 respectively. In these figures we've only plotted results where the error was less than the value itself.

If these estimates for the number of stable configurations are reasonable, and if the growth in the number of stable configurations is exponential, then fits from $N = 100, \dots, 180$ for

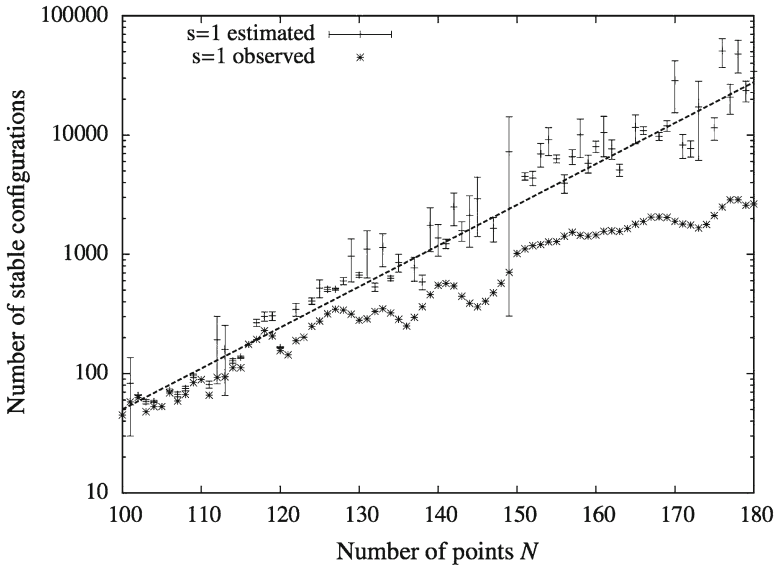


Fig. 6 The number of observed distinct stable configurations and estimates for the total number of distinct stable configurations as a function of N for $s = 1$

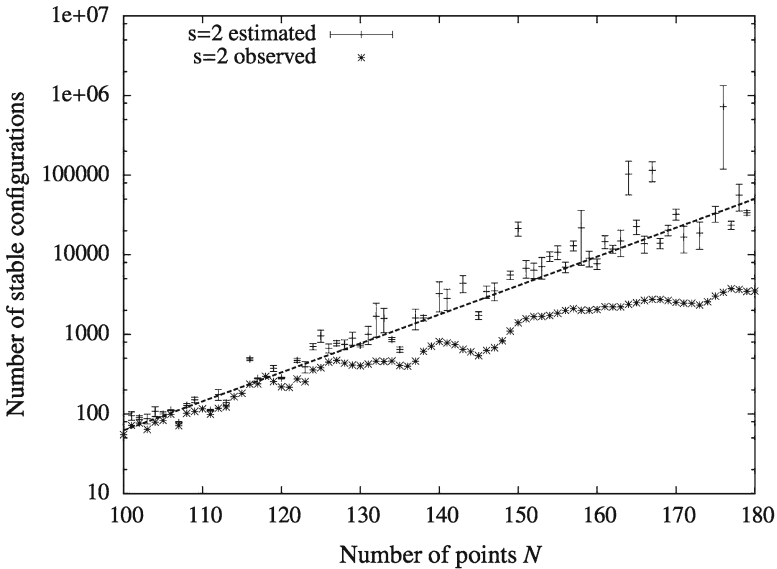


Fig. 7 The number of observed distinct stable configurations and estimates for the total number of distinct stable configurations as a function of N for $s = 2$

the number of stable configurations as a function of N and s indicate that the number of stable configurations as a function of N and s is given by

$$M(N, s) = C_s N^{e_s},$$

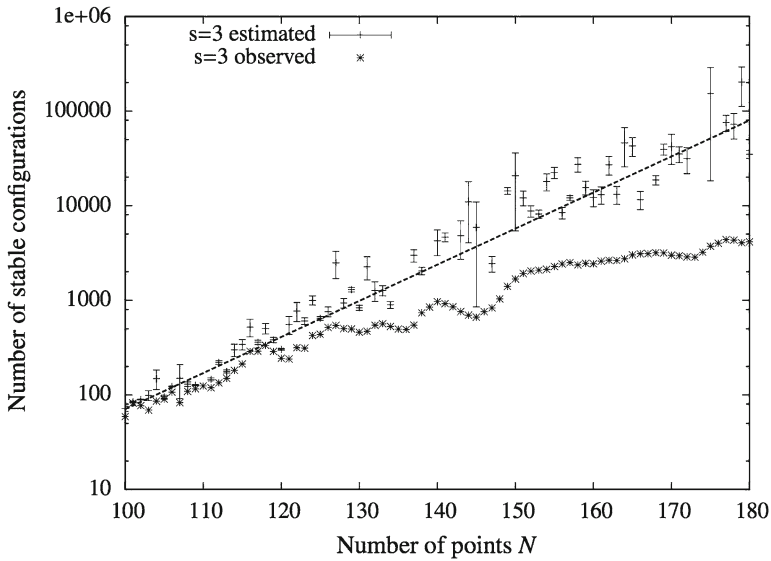


Fig. 8 The number of observed distinct stable configurations and estimates for the total number of distinct stable configurations as a function of N for $s = 3$

where e_s and C_s are given by

$$\begin{aligned}
 e_0 &= 0.0741345 \pm 0.002804 & C_0 &= \exp(-3.91164 \pm 0.3044), \\
 e_1 &= 0.0789298 \pm 0.00176 & C_1 &= \exp(-3.97635 \pm 0.1992), \\
 e_2 &= 0.0836987 \pm 0.002186 & C_2 &= \exp(-4.23711 \pm 0.2583), \\
 e_3 &= 0.0878486 \pm 0.001698 & C_3 &= \exp(-4.52585 \pm 0.1882).
 \end{aligned}$$

If we perform a similar fit to the number of observed configurations for $s = 1$, as opposed to the number of estimated configurations, we obtain $M(N, 1) = (0.31701 \pm .1) \exp(0.0518 \pm 0.0012 N)$, which is similar to Erber’s and Hockney’s estimate of $M(N, 1) = 0.382 \exp(0.0497N)$ noted above. This growth is considerably slower than the growth in the estimated number of stable configurations, which we feel is likely closer to the actual growth in the number of stable configurations.

5 Conclusions

When searching for isomorphisms between a set of configurations of points on a sphere, the use of a simple invariant under isometry, the discrete energy E_s , quickly filtered out many configurations as not-isometric. After this a more comprehensive invariant under isometry, the graph of non-degenerate extremal triangulations, was extremely effective.

It is reasonable to express concern over the number of assumptions and over the sensitivity of N_f in Eq. (4) to the other parameters. The defensible conclusion is that there are substantially more stable configurations than those we observed, and just as performing enough trials to observe the configuration with the lowest energy is a formidable technical challenge, so too is finding all the stable configurations.

Acknowledgments The authors are grateful to Mark Ellingham for his clear explanation of Algorithm 2. The authors are also grateful to the referees for their suggested changes to the manuscript. The work of Matthew Calef was performed under the auspices of the National Nuclear Security Administration of the US Department of Energy at Los Alamos National Laboratory under Contract No. DE-AC52-06NA25396. LA-UR-14-27638. The work of Alexia Schulz is sponsored by the Assistant Secretary of Defense for Research & Engineering under Air Force Contract #FA8721-05-C-0002. Opinions, interpretations, conclusions and recommendations are those of the authors and are not necessarily endorsed by the United States Government.

References

1. Barber, C., Dobkin, D., Huhdanpaa, H.: The Quickhull algorithm for convex hulls. *ACM Trans. Math. Softw.* **22**(4), 469–483 (1996)
2. Borodachov, S., Hardin, D., Saff, E.: Asymptotics for discrete weighted minimal energy problems on rectifiable sets. *Trans. Am. Math. Soc.* **360**(3), 1559–1580 (2008)
3. Calef, M., Griffiths, W., Schulz, A., Fichtl, C., Hardin, D.: Observed asymptotic differences in energies of stable and minimal point configurations on \mathbb{S}^2 and the role of defects. *J. Math. Phys.* **54**(10), 101901 (2013)
4. Demmel, J., Hida, Y.: Accurate and efficient floating point summation. *SIAM J. Sci. Comput.* **25**(4), 1214–1248 (2003)
5. Efron, B., Thisted, R.: Estimating number of unseen species—how many words did Shakespeare know? *Biometrika* **63**(3), 435–447 (1976)
6. Erber, T., Hockney, G.: Equilibrium-configurations of n equal charges on a sphere. *J. Phys. A* **24**(23), L1369–L1377 (1991)
7. Erber, T., Hockney, G.M.: Comment on “method of constrained global optimization”. *Phys. Rev. Lett.* **74**(8), 1482 (1995)
8. Erber, T., Hockney, G.: Complex systems: equilibrium configurations of n equal charges on a sphere ($2 \leq n \leq 112$). *Adv. Chem. Phys.* **98**, 495–594 (1997)
9. Gale, W., Sampson, G.: Good–Turing frequency estimation without tears. *J. Quant. Linguist.* **2**(3), 217–237 (1995)
10. Good, I.: The population frequencies of species and the estimation of population parameters. *Biometrika* **40**(3–4), 237–264 (1953)
11. Hardin, D., Saff, E.: Minimal riesz energy point configurations for rectifiable d -dimensional manifolds. *Adv. Math.* **193**, 174–204 (2005)
12. Higham, N.: The accuracy of floating-point summation. *SIAM J. Sci. Comput.* **14**(4), 783–799 (1993)
13. Hoare, M.R., McInnes, J.: Statistical-mechanics and morphology of very small atomic clusters. *Faraday Discuss.* **61**, 12–24 (1976)
14. Kuijlaars, A., Saff, E.: Asymptotics for minimal discrete energy on the sphere. *Trans. Am. Math. Soc.* **350**(2), 523–538. MR 1458327 (98e:11092) (1998)
15. Lakhbab, H., El Bernoussi, S.: A new hybrid approach for tackling Thomson problem. In: Aboutajdine, D., Skalli, A., Benchekroun, B., Artiba, A. (eds.) *Proceedings of the 2013 International Conference on Industrial Engineering and Systems Management (IESM)* (2013)
16. Landkof, N.: *Foundations of Modern Potential Theory*. Springer, New York (1973)
17. Lins, S.: A sequence representation for maps. *Discrete Math.* **30**(3), 249–263. MR MR573640 (81h:68057) (1980)
18. Melnyk, T., Knop, O., Smith, W.: Extremal arrangements of points and unit charges on a sphere—equilibrium configurations revisited. *Can. J. Chem.* **55**(10), 1745–1761 (1977)
19. Morris, J., Deaven, D., Ho, K.: Genetic-algorithm energy minimization for point charges on a sphere. *Phys. Rev. B* **53**(4), R1740–R1743 (1996)
20. Pólya, G., Szegő, G.: The transfinite diameter (capacity constants) of even and spatial point sets. *Journal Fur Die Reine Und Angewandte Mathematik* **165**, 4–49 (1931) (in German)
21. Smale, S.: Mathematical problems for the next century, *Gac. R. Soc. Mat. Esp.* **3**(3), 413–434 (2000), Translated from *Math. Intelligencer* 20(2), 7–15 (1998) [MR1631413 (99h:01033)] by M. J. Alcón. MR MR1819266
22. Stillinger, F.H., Weber, T.A.: Hidden structure in liquids. *Phys. Rev. A* **25**(2), 978–989 (1982)
23. Thomson, J.: On the structure of the atom: an investigation of the stability and periods of oscillation of a number of corpuscles arranged at equal intervals around the circumference of a circle: with application of the results to the theory of atomic structure. *Philos. Mag. Ser.* **7**(39), 237–265 (1904)

24. Wales, D., Ulker, S.: Structure and dynamics of spherical crystals characterized for the Thomson problem. *Phys. Rev. B* **74**(21), 212101 (2006)
25. Wales, D., McKay, H., Altschuler, E.: Defect motifs for spherical topologies. *Phys. Rev. B* **79**(22), 224115 (2009)